QCD transition line from lattice simulations

Claudia Ratti

University of Houston

Collaborators: Szabolcs Borsanyi, Zoltan Fodor, Jana Guenther, Ruben Kara, Sandor Katz, Paolo Parotto, Attila Pasztor, Kalman Szabo

S. Borsanyi et al., 2002.02821

Motivation

- Map the phase diagram of strongly interacting matter
- Locate the critical point
- Find it in experiments

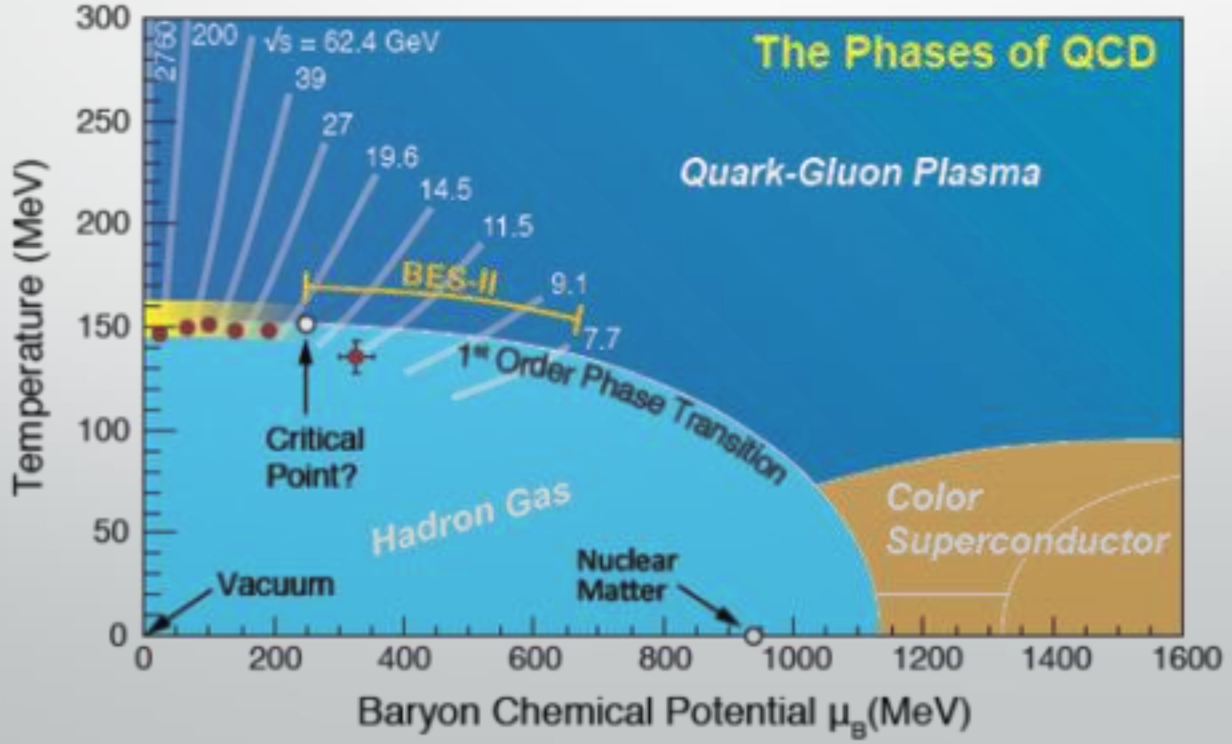

Second Beam Energy Scan (BESII) at RHIC

- Running in 2019-2021
- 24 weeks of runs each year
- Beam Energies have been chosen to keep the μ_B step ~50 MeV
- Chemical potentials of interest: μ_B/T~1.5…4

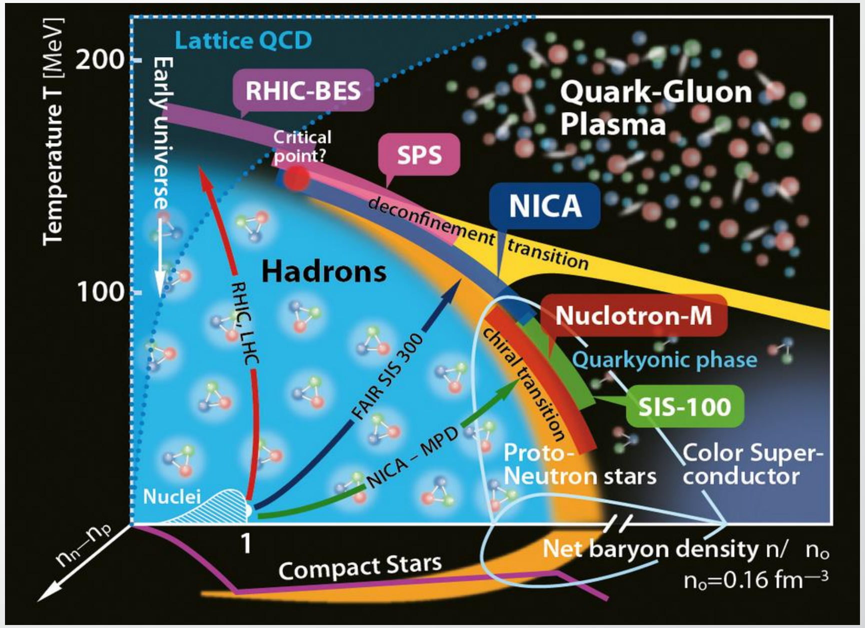

$\sqrt{s}$ (GeV)	19.6	14.5	11.5	9.1	7.7	6.2	5.2	4.5
μ_B (MeV)	205	260	315	370	420	487	541	589
# Events	400M	300M	230M	160M	100M	100M	100M	100M

Collider (19.6–9.1 GeV) | Fixed Target (7.7–4.5 GeV)

Comparison of the facilities

Compilation by D. Cebra

Facilty	RHIC BESII	SPS	NICA	SIS-100 SIS-300	J-PARC HI
Exp.:	STAR +FXT	NA61	MPD + BM@N	CBM	JHITS
Start:	2019-20 2018	2009	2020 2017	2022	2025
Energy: $\sqrt{s_{NN}}$ (GeV)	7.7– 19.6 2.5-7.7	4.9-17.3	2.7 - 11 2.0-3.5	2.7-8.2	2.0-6.2
Rate: At 8 GeV	100 HZ 2000 Hz	100 HZ	<10 kHz	<10 MHZ	100 MHZ
Physics:	CP&OD	CP&OD	OD&DHM	OD&DHM	OD&DHM
	Collider Fixed target	Fixed target Lighter ion collisions	Collider Fixed target	Fixed target	Fixed target

CP=Critical Point OD= Onset of Deconfinement DHM=Dense Hadronic Matter

How can lattice QCD support the experiments?

- Equation of state
  - Needed for hydrodynamic description of the QGP
- QCD phase diagram
  - Transition line at finite density
  - Constraints on the location of the critical point
- Fluctuations of conserved charges
  - Can be simulated on the lattice and measured in experiments
  - Can give information on the evolution of heavy-ion collisions
  - Can give information on the critical point

Lattice QCD

- Best first principle-tool to extract predictions for the theory of strong interactions in the non-perturbative regime
- Uncertainties:
  - Statistical: finite sample, error
  - Systematic: finite box size, unphysical quark masses
- Given enough computer power, uncertainties can be kept under control
- Results from different groups, adopting different discretizations, converge to consistent results
- Unprecedented level of accuracy in lattice data

Sign problem

- The QCD path integral is computed by Monte Carlo algorithms which samples field configurations with a weight proportional to the exponential of the action

$$Z(\mu_B, T) = \mathrm{Tr}\left(e^{-\frac{H_{QCD} - \mu_B N_B}{T}}\right) = \int \mathcal{D}U e^{-S_G[U]} \det M[U, \mu_B]$$

- det$M[\mu_B]$ complex → Monte Carlo simulations are not feasible

- We can rely on a few approximate methods, viable for small μ_B/T:
  - Taylor expansion of physical quantities around $\mu_B=0$ (Bielefeld-Swansea collaboration 2002; R. Gavai, S. Gupta 2003)
  - Simulations at imaginary chemical potentials (plus analytic continuation)(Alford, Kapustin, Wilczek, 1999; de Forcrand, Philipsen, 2002; D'Elia, Lombardo 2003)

Methods

$$\frac{T_c(\mu_B)}{T_c(\mu_B=0)} = 1 - \kappa_2 \left(\frac{\mu_B}{T_c(\mu_B)}\right)^2 - \kappa_4 \left(\frac{\mu_B}{T_c(\mu_B)}\right)^4$$

- Two ways of extracting the phase transition line:
  - Taylor expansion of observables around $\mu_B=0$
  - Simulations at imaginary chemical potential + analytical continuation
- Two choices for the other chemical potentials:
  - $\mu_B \neq 0$, $\mu_S=\mu_Q=0$
  - μ_S and μ_Q are functions of T and μ_B to match the experimental constraints:

$$\langle n_S \rangle = 0 \qquad \langle n_Q \rangle = 0.4 \langle n_B \rangle$$

State of the art

- From direct simulations at μ_B=0:
  - $T_c(\mu_B=0)$=(156.5±1.5) MeV
  - K_2=0.012±0.004
  - K_4=0.000±0.004

HotQCD: PRL (2018)

Compilation by F. Negro

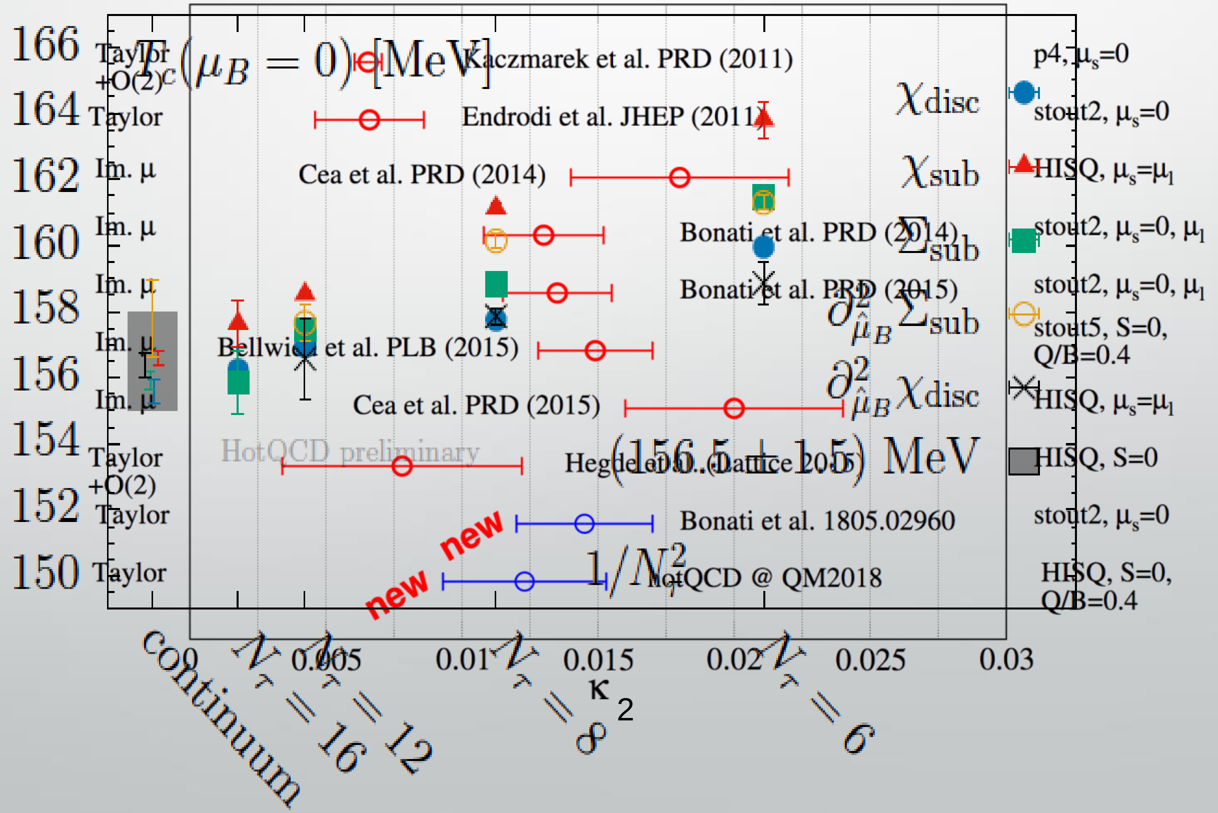

Our method: simulations at imaginary μ_B

- Simulation landscape

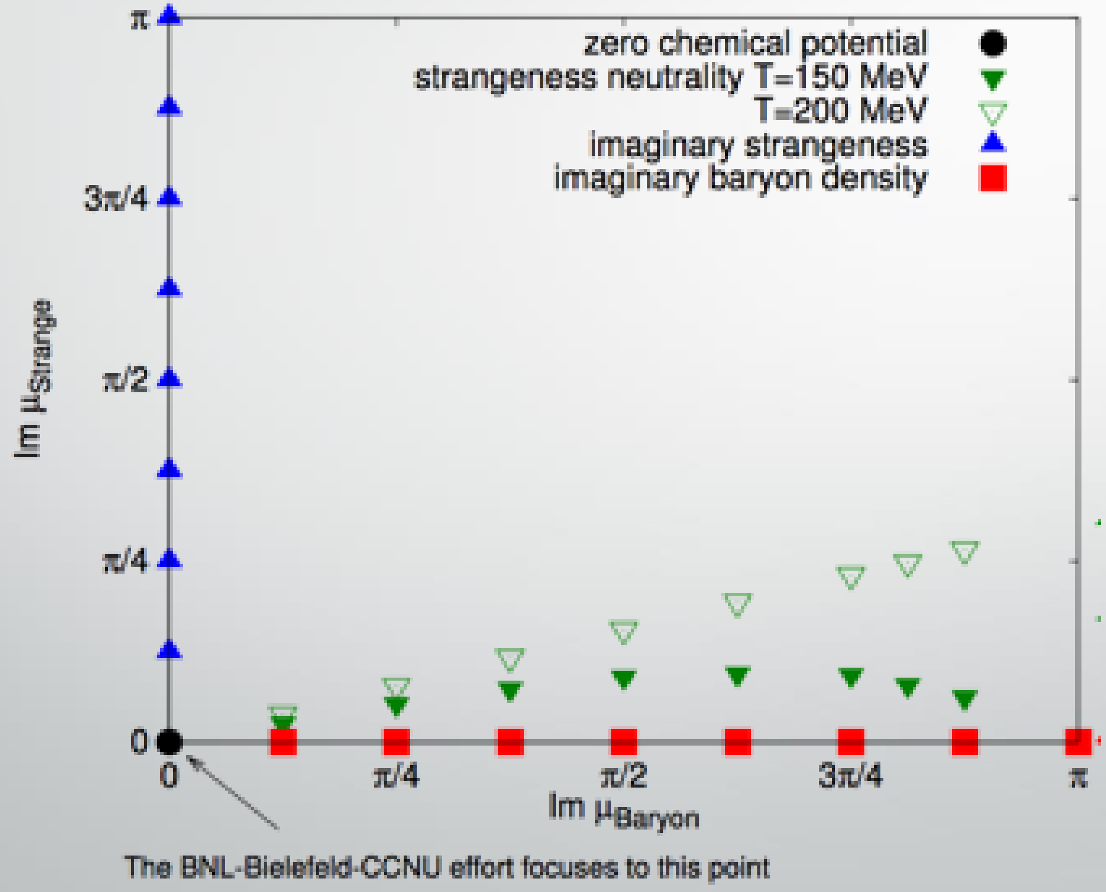

Common technique: [de Forcrand, Philipsen, deForcrand:2002hgr], [Bonati et al., Bonati:2015bha], [Cea et al., Cea:2015cya], [D'Elia et al., DElia:2016jqh], [Bonati et al., Bonati:2018nut]

Observables

- We consider the following observables:

$$\langle\bar{\psi}\psi\rangle = -\left[\langle\bar{\psi}\psi\rangle_T - \langle\bar{\psi}\psi\rangle_0\right]\frac{m_{\mathrm{ud}}}{f_\pi^4}\,,$$

$$\chi = \left[\chi_T - \chi_0\right]\frac{m_{\mathrm{ud}}^2}{f_\pi^4}\,, \quad \text{with}$$

$$\langle\bar{\psi}\psi\rangle_{T,0} = \frac{T}{V}\frac{\partial \log Z}{\partial m_{\mathrm{ud}}} \quad \chi_{T,0} = \frac{T}{V}\frac{\partial^2 \log Z}{\partial m_{\mathrm{ud}}^2}$$

- The peak height of the susceptibility indicates the strength of the transition

- The peak position in temperature serves as a definition for the chiral cross-over temperature

Observables

- Plan:
  - Calculate these two observables at finite imaginary μ_B and finite temperature T
  - Use the shift of these observables as a function of imaginary μ_B to determine T_c, K_2 and K_4

S. Borsanyi et al., 2002.02821

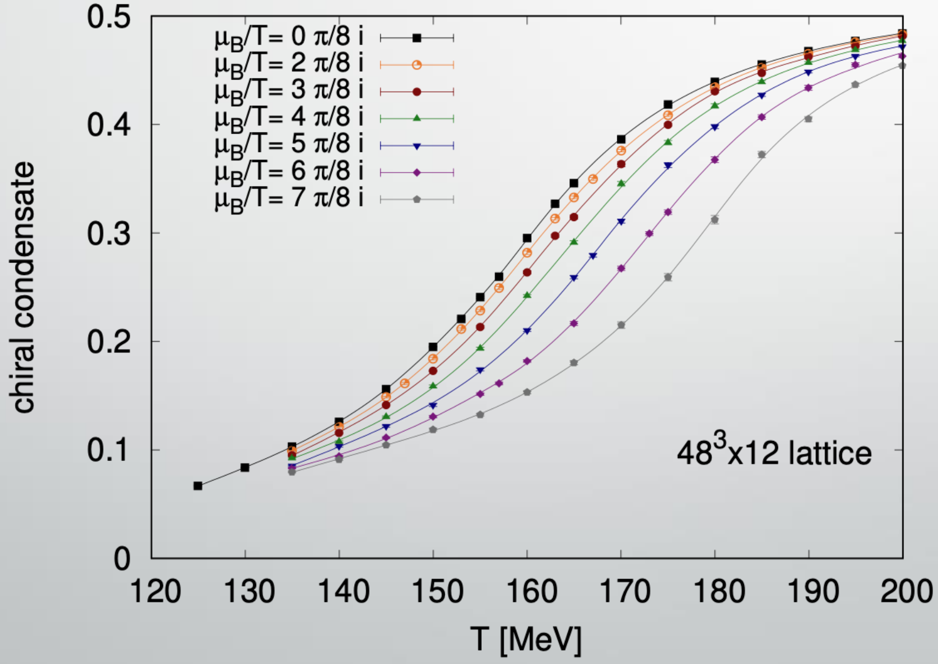

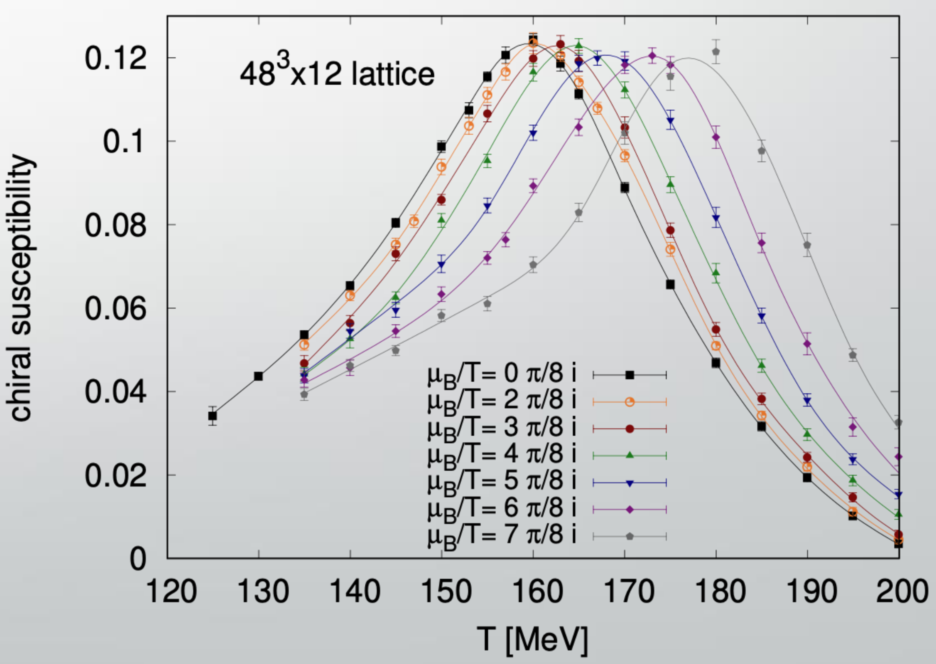

Observables

- Observation
  - When we plot the chiral susceptibility as a function of the chiral condensate, we observe a very weak chemical potential dependence

S. Borsanyi et al., 2002.02821

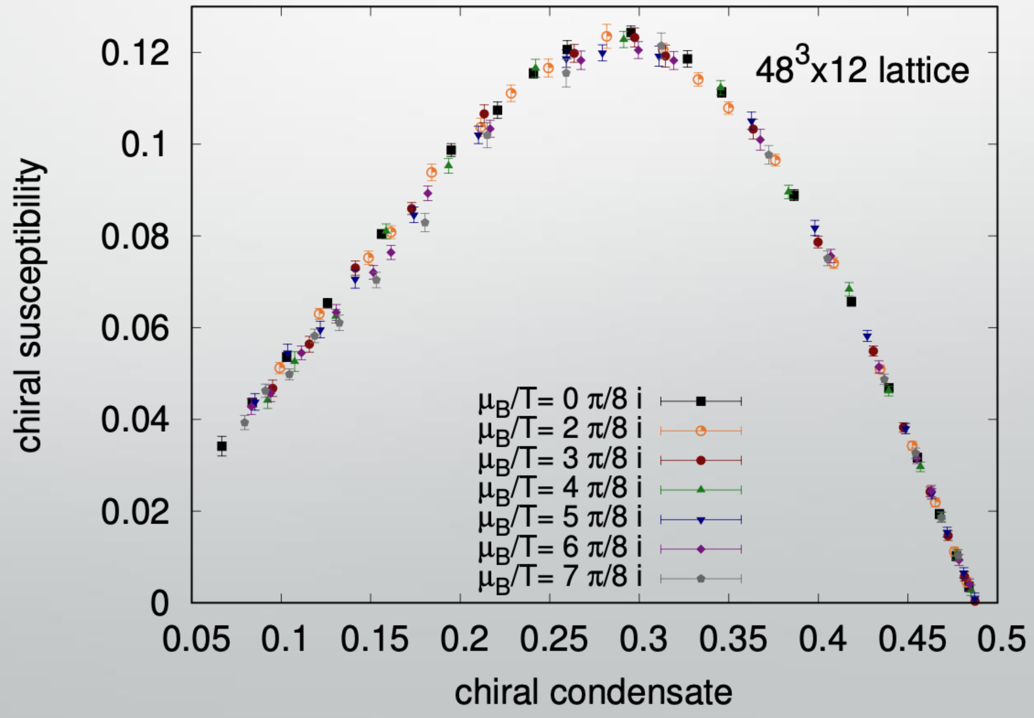

Procedure

- Find the peak in the curve $\chi(\langle\bar{\psi}\psi\rangle)$ through a low-order polynomial fit for each N_t and imaginary μ_B. This yields $\langle\bar{\psi}\psi\rangle_c$
- Use an interpolation of $\langle\bar{\psi}\psi\rangle(T)$ to convert $\langle\bar{\psi}\psi\rangle_c$ to T_c for each N_t and imaginary μ_B.
- Perform a fit of $T_c(N_t, \mathrm{Im}\mu_B/T_c)$ to determine the coefficients K_2 and K_4
- This leads to 2^8=256 independent analyses

Results

$$T_c(LT=4,\mu_B=0) = 158.0 \pm 0.6\ \text{MeV}$$
$$\kappa_2 = 0.0153 \pm 0.0018\ ,$$
$$\kappa_4 = 0.00032 \pm 0.00067$$

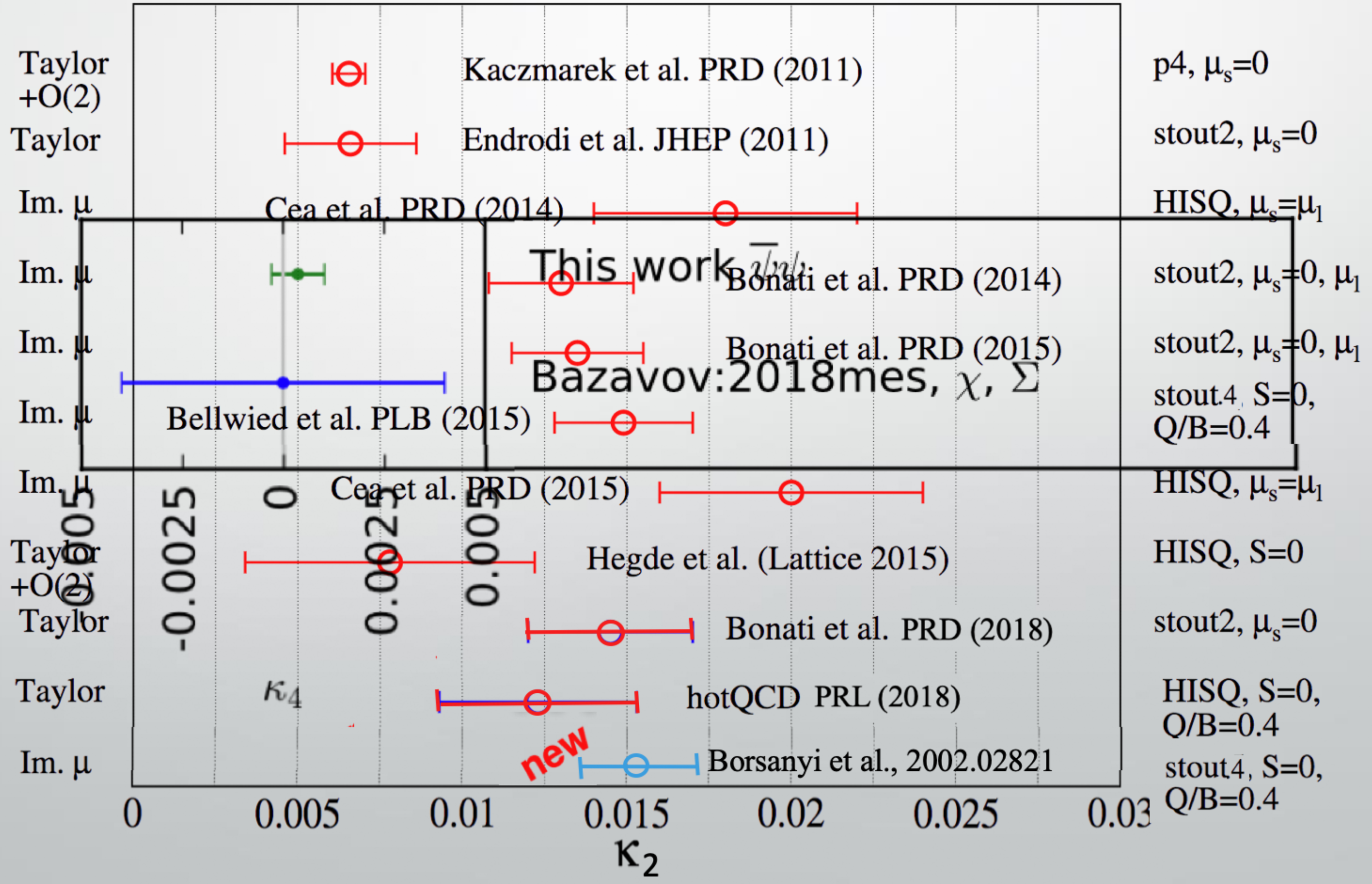

Results

S. Borsanyi et al., 2002.02821

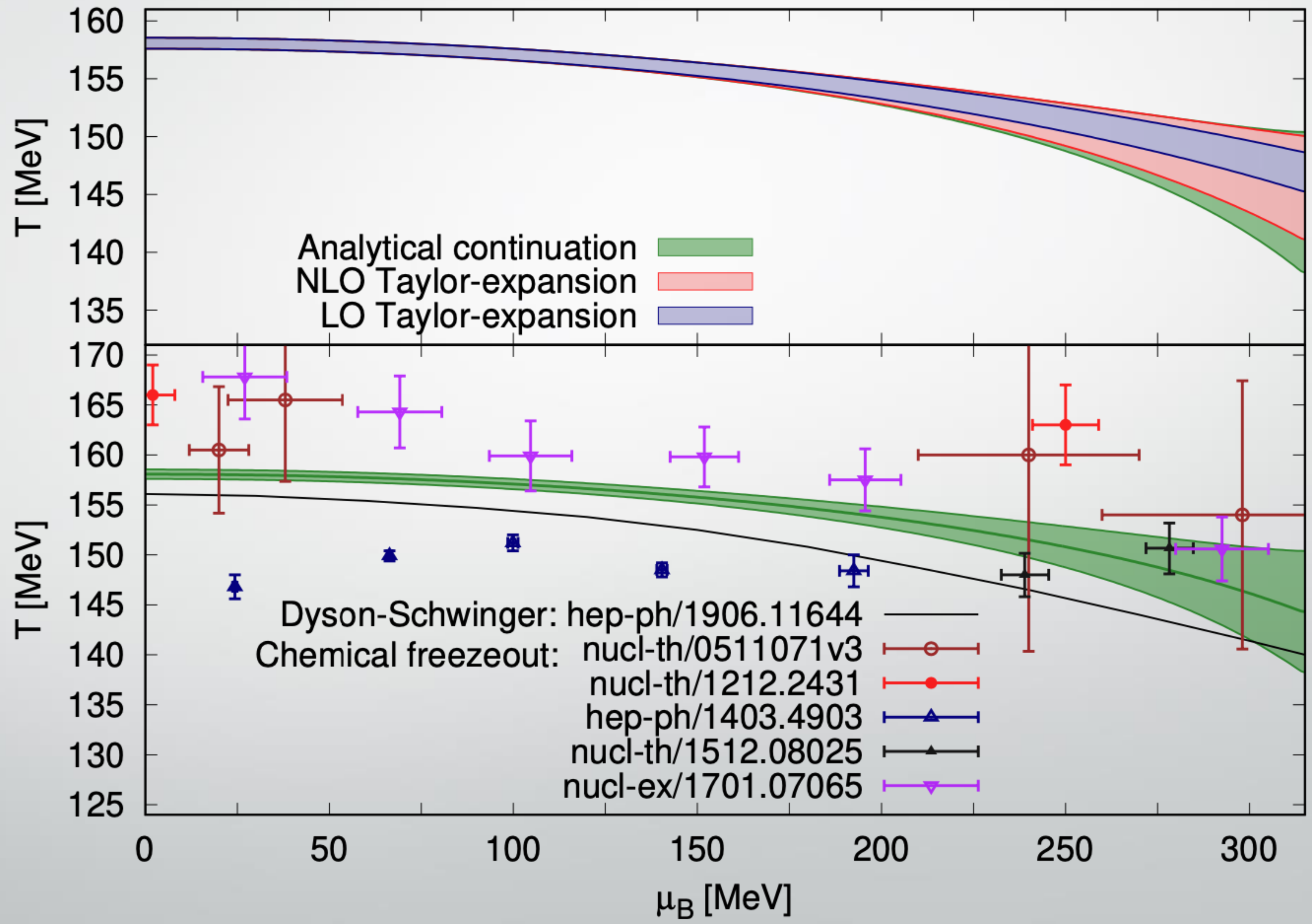

Width of the transition

- Natural definition: second derivative of the susceptibility at T_c

$$(\Delta T)^2 = -\chi(T_c)\left[\frac{d^2}{dT^2}\chi\right]^{-1}_{T=T_c}$$

- This turns out to be noisy, so we replace it by σ, a proxy for ΔT defined as:

$$\langle\bar{\psi}\psi\rangle(T_c \pm \sigma/2) = \langle\bar{\psi}\psi\rangle_c \pm \Delta\langle\bar{\psi}\psi\rangle/2$$

with $\langle\bar{\psi}\psi\rangle_c = 0.285$ and $\Delta\langle\bar{\psi}\psi\rangle = 0.14$

- The exact range is chosen such that σ coincides with ΔT at zero and imaginary μ_B.

Width of the transition

S. Borsanyi et al., 2002.02821

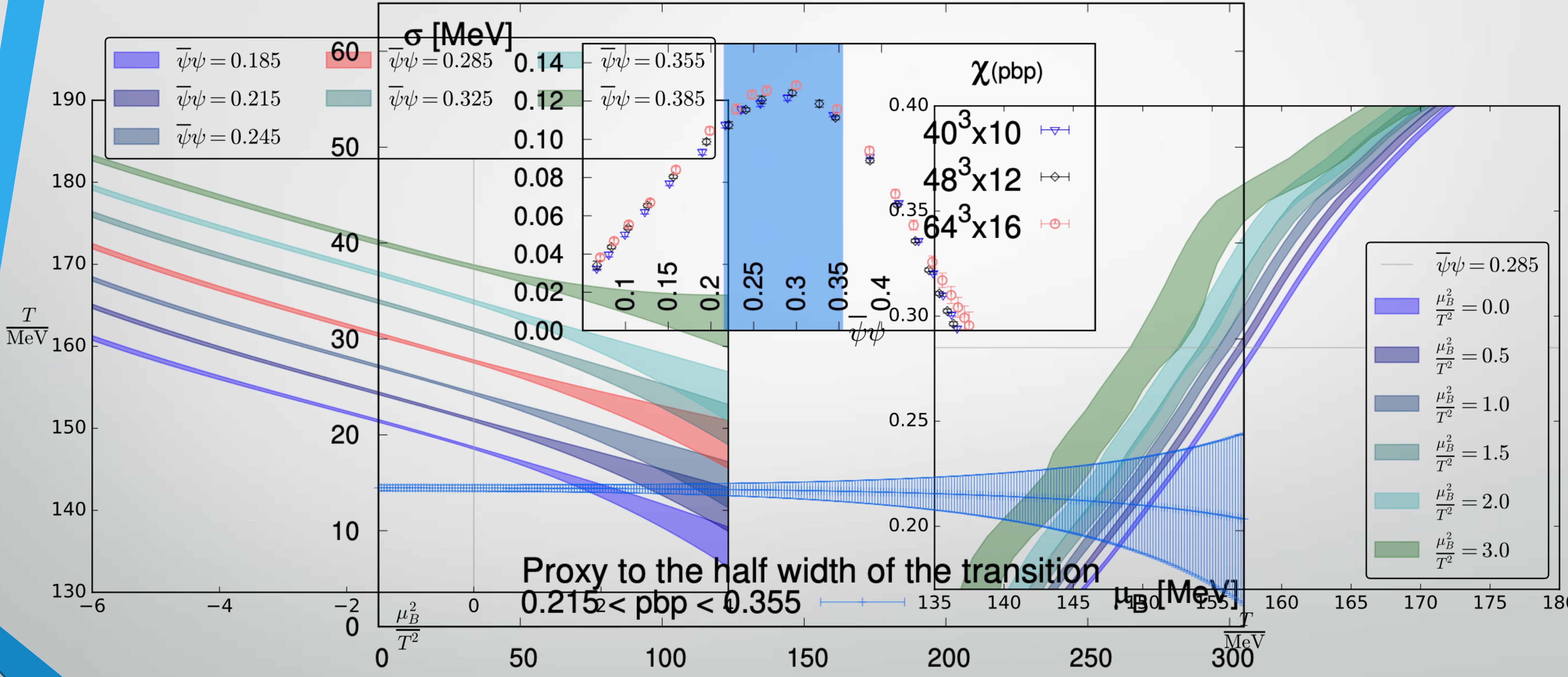

- The width of the transition is constant up to μ_B~300 MeV

Strength of the transition

- Height of the peak of the chiral susceptibility at the crossover temperature: proxy for the strength of the crossover

S. Borsanyi et al., 2002.02821

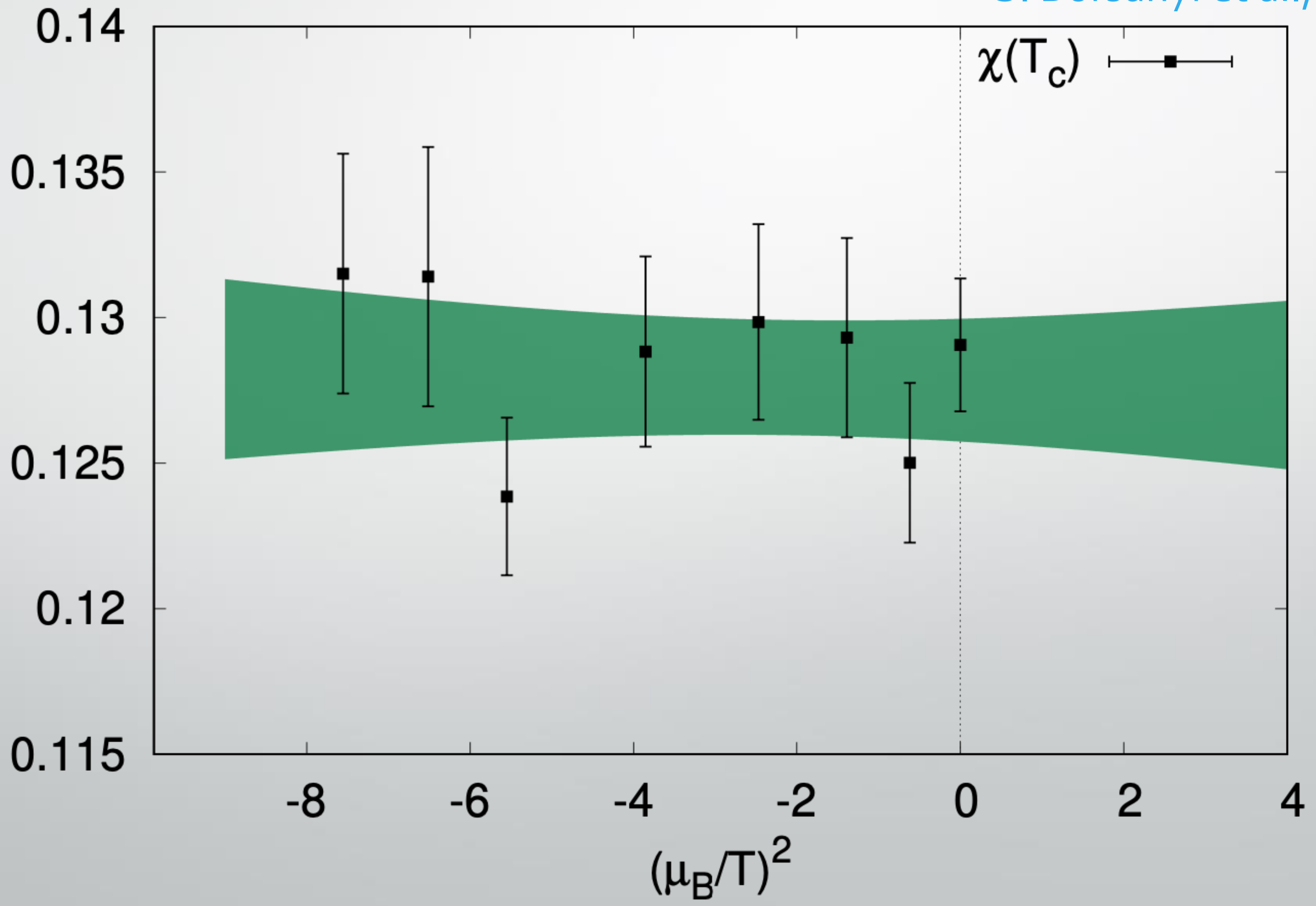

Conclusions

- We obtained the most accurate results for the QCD transition line so far
- The curvature at μ_B=0 is very small. Its NLO correction is compatible with zero
- The width of the phase transition remains constant up to μ_B~300 MeV
- The strength of the phase transition remains constant up to μ_B~300 MeV
- We see no sign of criticality in the explored range

Backup slides

Number of analyzed configurations

T [MeV]	$40^3 \times 10$ lattice, μ_B^I/T = 0.000	0.785	1.178	1.570	1.963	2.356	2.553	2.749
135	20159	2042	2518	3255	2384	2690	4373	3728
140	15898	8904	2555	3260	2407	2692	4381	3815
145	9638	10061	2609	3259	2425	4444	4545	3883
150	9382	9710	7192	6951	4840	2729	4516	3839
155	9663	6235	4812	9966	8654	2735	4382	5713
160	9783	6223	4680	10128	9001	7695	4595	5577
165	19507	11576	2799	9806	9774	10379	4676	5920
170	16196	12332	5634	4226	10300	11591	4815	6035
175	10593	13316	1540	7110	5287	11453	4875	4271
180	10007	12950	1653	8313	2096	3279	5256	4501
185	5492	1766	5959	6841	2235	3521	5666	4877
190	9938	1855	1878	6891	2357	7636	6131	5240
195	6951	1473	1155	3426	6087	7074	4823	3062
200	9765	1518	2016	8160	6157	6609	5081	3244

Number of analyzed configurations

$48^3 \times 12$ lattice								
T [MeV]	μ_B^I/T							
	0.000	0.785	1.178	1.570	1.963	2.356	2.553	2.749
135	27681	5925	2632	4247	3459	4067	5130	5312
140	27723	5806	4051	4187	3471	4015	5174	5275
145	27147	5677	9596	6914	6018	5125	5326	5397
150	18137	5704	15529	7598	3587	6564	5445	5429
155	27359	5939	7350	7651	8432	6540	5390	5670
160	17460	6350	6888	7912	11561	9062	5386	5695
165	27257	7043	5827	9574	13957	7982	5436	5826
170	8833	7916	5527	6533	9055	9418	5621	6052
175	16805	8777	4338	3912	5240	7888	5771	5965
180	17182	9743	3367	4347	5924	7281	6230	6311
185	14146	10649	3618	4583	6392	7750	6640	6805
190	18668	11405	3851	4934	6847	3598	6982	7171
195	14972	12223	4023	4730	6025	1702	6152	7541
200	20991	12942	4258	5038	6325	1736	6608	7940

Number of analyzed configurations

$64^3 \times 16$ lattice								
T [MeV]	μ_B^I/T							
	0.000	0.785	1.178	1.570	1.963	2.356	2.553	2.749
135	23194	1909	5659	6288	3927	4400	3100	3261
140	13587	2813	6632	4915	4856	4352	3089	3238
145	13682	2679	7157	5791	4713	5965	2991	3310
150	13697	2577	9095	5777	4346	4286	2902	3406
155	14164	2865	7886	6900	4706	4411	3005	3114
160	14465	2689	9136	6870	4980	6124	3439	3129
165	14983	7714	9809	7786	6572	7286	3673	3375
170	15594	8360	12324	6378	5313	7205	3927	3256
175	16362	9380	15056	6948	4911	8441	3382	3361
180	16960	10453	8064	6966	5251	9173	3290	3546
185	7689	3504	7844	7120	5723	8831	3602	3320
190	33373	3416	5777	7543	6077	6306	4879	3678
195	8918	4389	5931	7895	5841	6858	5204	3835
200	14308	4770	6049	8336	5785	7289	2602	4035